GEOGRAPHICAL ANALYSIS

ORIGINAL ARTICLE

Monitoring Precipitation Patterns and their Direct Impacts on Vegetation and Water Indices for Mangura Nala Watershed using Geospatial Approaches in Bihar State, India

Rashmi Bala[1]*, M A Mohammed-Aslam[1], N Harishnaika[2], M Arpitha[2]

1 *Department of Geology, Central University of Karnataka, Kalaburagi, Karnataka, India*
2 *Department of Applied Geology, Kuvempu University, Karnataka, India*

OPEN ACCESS

Received: 26.05.2025
Accepted: 10.08.2025
Published: 01.12.2025

Citation: Bala R, Mohammed-Aslam MA, Harishnaika N, Arpitha M. (2025). Monitoring Precipitation Patterns and their Direct Impacts on Vegetation and Water Indices for Mangura Nala Watershed using Geospatial Approaches in Bihar State, India. Geographical Analysis. 14(2): 14-21. https://doi.org/10.53989/bu.ga.v14i2.25.86

* **Corresponding author**.
balarashmi1511@gmail.com

Funding: None

Competing Interests: None

Published By Bangalore University, Bengaluru, Karnataka

ISSN
Print: 2319-5371
Electronic: XXXX-XXXX

Abstract

Among the several impacts of climate change, variation in global and regional precipitation patterns is evident in the current scenario. Spatiotemporal alterations, including a rise in frequency and severity of extreme weather events, are manifested in the occurrence of wide-scale droughts, floods, and heavy rainfall. Since climate change is inevitable, studying and monitoring shifts in precipitation patterns can help us cope with the adverse effects of climate change. To understand this effect at a regional scale, a study has been conducted on the Mangura Nala watershed to monitor the precipitation pattern and their impact on vegetation and water indices. In this evaluation process, a 2013-2023 gridded precipitation dataset, MODIS satellite data sets, and Landsat-8 satellite data have been incorporated to examine precipitation, vegetation, and water body trends in the study region. The index called Normalized Difference Water Index (NDWI) has been used to fathom the distribution and condition of water bodies in the study region, while the Enhanced Vegetation Index (EVI) and Normalized Difference Vegetation Index (NDVI) indices were used to monitor the vegetation conditions in the region.

Keywords: NDWI; EVI; NDVI; Precipitation; Mangura Nala Watershed

1 Introduction

Hydrological cycle explains the exchange and movement of water through the atmosphere, hydrosphere, lithosphere, and biosphere, and this cycle depends on rainfall to a great extent[(1)]. The spatiotemporal variation in rainfall patterns due to climate change has impacts ranging from water availability, environment, agriculture, to human civilization[(2)]. Shifts in parameters of precipitation, such as quantity, duration, and intensity, possibly result from spatial-temporal variations in rainfall patterns and might also influence soil moisture, streamflow patterns, and the likelihood of droughts and floods[(3–9)]. Many researchers have documented the spatiotemporal fluctuations in precipitation patterns throughout India, observing an increase in pre-monsoon rains and a rise in dry spells nationally. Although the yearly rainfall trend is negative or declining, there is a

non-significant increase in the percentage of days with heavy rainfall[10–13]. The primary components in an ecosystem are plants, which are essential at every stage of the ecosystem. Local vegetation is a determining factor in balancing climate-related environmental changes and ensuring its stability[14,15]. Growth and distribution of flora are significantly influenced by rainfall, because of which any variation in its pattern may severely affect plant growth. The mutability of indices such as NDVI and EVI is immensely impacted by climate change, which leads to fluctuations in rainfall[16,17]. When it comes to vegetation indices, viz. NDVI and EVI of plants, incessant rainfall results in their great increase in their values. It signifies that these indices can be used as indicators of ecological change and vegetation growth[18–20]. Normalized Difference Vegetation Index (NDVI) can be employed to examine tree cover, its canopy, along with its greenness, which also helps in the assessment of the phenophases of extensive plant regions[21,22]. Apart from NDVI, other indices are also used to assess different ecological components, such as water. It is commonly accepted among researchers that the Normalized Difference Water Index (NDWI) could be a source of digital information from remote sensing for assessing the clarity of water bodies[23,24]. To fathom the distribution and condition of open water features, the NDWI, as an excellent technique, can be well used. It also enhances their traceability through satellite-based remote sensing[25]. Remote sensing techniques always play a significant role in providing accurate information within a stipulated time[26–28]. Increasing focus and highlighting visibility of water, the NDWI eliminates the presence of soil and terrestrial vegetation features using multispectral bands of EMR, including visible green light and reflected near-infrared radiation. Presence of water can sometimes be masked by the presence of other features in the vicinity; therefore, to distinguish water, NDWI values should have a threshold that could be determined using mathematical equations but could also be subjective, thus leading to over or underestimation of the target feature[29]. Given the importance of indices such as NDVI and NDWI, they have been incorporated in studying the regional trends in precipitation patterns, and their impact on vegetation in the Mangura Nala watershed, involving rainfall analysis, water, and vegetation index models. In this study, spatiotemporal variation in rainfall patterns as well as the changes in the frequency and extremity of climatic events have also been included. A multi-pronged approach incorporating remote sensing technology has been utilized to determine the prevailing situation and distribution of the water bodies and vegetation cover in the study region.

2 Study Area

Mangura Nala Watershed has been considered for this study area. The watershed is situated in the southern part of Bihar State, India. The study area, which is the watershed, lies in two districts, namely Gayaji to a major extent and in Nawada to a minor extent. The region is well known for its diverse culture and is also recognized for its tourism. The Mangura Nala watershed covers an area of 278.47 sq. km and lies between latitudes 24°35'24"N to 24°55'51.6"N and longitudes 84°59'34.8"E to 85°31'1.2"E (Figure 1). According to Koeppen's climate classification, the area lies in Cwg, which indicates a subtropical humid climate (the average rainfall is approximately 1145.9 mm, and the temperature ranges from 23° C to 25° C).

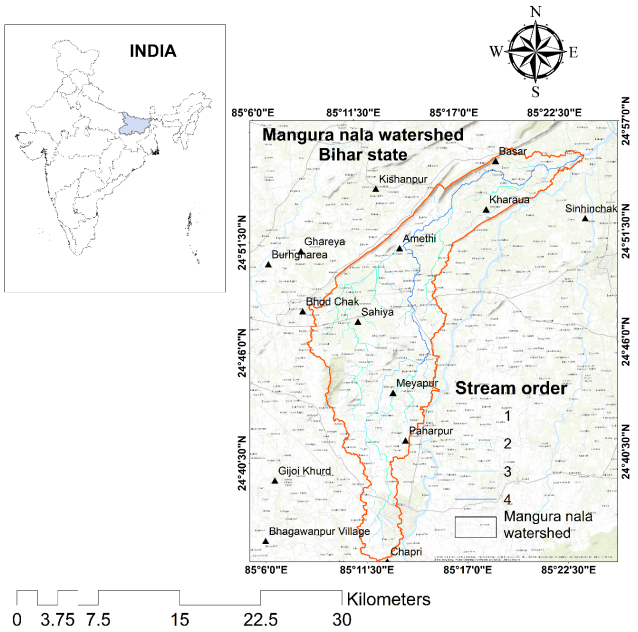

Fig. 1. Study Area with Geographic Information

3 Materials and Methods

The Google Earth Engine (GEE) includes a significant quantity of Earth observation commonly used systems, containing MODIS, Landsat, and Sentinel, as well as multiple geospatial platforms containing demographic and climatic data. The MODIS NDVI EVI, Sentinel-2A, and Landsat-8 satellite imagery were used in this study, with 2013 to 2023 as the imaging period. The precipitation data was taken from the USGS climate platform. ArcGIS and ERDAS Imagine GEE are used to perform the image classification and calculations. This investigation utilizes MODIS satellite data, which can be accessed on the appEEARS website. MODIS NDVI (16-Day L3 Global 250m- MOD13A1) was chosen because of its relationship with several ecological factors, data availability, and coverage over the research. For rainfall statistics, 15 stations in and around the watershed were used, as shown in Table 1 and Figure 2. An area at 250m and 500m resolutions in

Table 2 indicates the different satellites used for the analysis.

Table 1. Climatic average statistics of Mangura Nala watershed from 2013-2023

Sl. No	Stations	Longitude (°E)	Latitude (°N)	Rainfall (in mm)	Temperature (in °C)
1	Amethi	85.23	24.85	975.8	26.36
2	Basar	85.32	24.92	1013.0	26.04
3	Bhagawanpur	85.1	24.61	1112.5	25.52
4	Bhod Chak	85.14	24.8	1872.3	26.36
5	Burhgharea	85.11	24.84	1872.3	26.36
6	Ghareya	85.14	24.85	975.8	26.36
7	Gijoi Khurd	85.11	24.66	1112.5	25.52
8	Kishanpur	85.21	24.9	975.8	26.36
9	Mai	85.31	24.98	975.8	26.36
10	Paharpur	85.23	24.69	1112.5	25.52
11	Sahiya	85.19	24.79	975.8	26.36
12	Meyapur	85.22	24.73	1112.5	25.52
13	Kharaua	85.31	24.88	975.8	26.36
14	Sinhinchak	85.4	24.87	1013.0	26.04
15	Chapri	85.21	24.59	1112.5	25.52

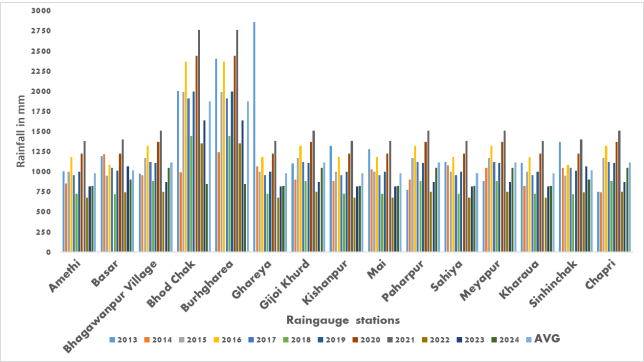

Fig. 2. Rainfall variation in individual rain gauge stations

Table 2. Satellite images used for analysis

MODIS Data Set	Units	Valid Range	Scale factor	Unit	Index range
250m 16 days NDVI	NDVI	-2000-10000	0.001	-	-1 to +1
250m 16 days EVI	EVI	2000-10000	0.001	-	-1 to +1
Landsat-8	NDWI	-	0.001	-	-1 to +1

3.1 Method for Extracting Satellite Images

Satellite data was obtained from online archives and pre-processed with atmospheric, geometric, and picture mosaic corrections. These images were resampled to a spatial resolution of 30 m using the average resampling method in ArcGIS (version 10.8). To study the condition of water bodies in the study area, Normalized Difference Water Index (NDWI), was used to generate streams from satellite data. Apart from NDWI, two other indices were also used, namely, Normalized Difference Vegetation Index (NDVI) and Enhanced Vegetation Index (EVI).

3.2 Normalized Difference Water Index (NDWI)

It is an index method used in remote sensing analysis of satellite imagery to identify open water features[30]. The method involves two bands from the EMR spectrum, namely, near-infrared (NIR) and visible green (GREEN) spectral bands. The NDWI can be calculated using the Equation (1) as follows:

$$\mathrm{NDWI} = (\mathrm{GREEN} - \mathrm{NIR})/(\mathrm{GREEN} + \mathrm{NIR}) \quad (1)$$

3.3 Normalized Difference Vegetation Index (NDVI)

NDVI is a very popular index method employed for evaluation of the vegetation conditions through remote sensing and satellite imagery[31]. The spectral bands used in the computation of NDVI are NIR (near-infrared) and red bands of satellite imagery such as Landsat. It can be calculated using Equation (2) as mentioned below:

$$NDVI = \frac{\rho_{\mathrm{nir}} - \rho_{\mathrm{red}}}{\rho_{\mathrm{nir}} + \rho_{\mathrm{red}}} \quad (2)$$

The normal range of NDVI values lies between -1.0 to +1.0. The NDVI classifications are shown in Table 3. It is commonly observed that the value range of NDVI for non-vegetated surfaces hovers between 0.1 (NIR < Red) to as high as 0.9, as determined by plants and other Earth's surface components. Factors contributing to higher NDVI values include increased green biomass, advantageous seasonal shifts, and beneficial rainfall[32].

3.4 Enhanced Vegetation Index (EVI)

This index can be well employed to assess the density and health of vegetation, mainly in densely vegetated areas. It is more susceptible to biomass, atmospheric background, and soil quality than the Normalized Difference Vegetation Index (NDVI), yet it is still an improvement. EVI calculates a number using the blue, red, and NIR (near-infrared) bands; values closer to 1 denote healthy vegetation. The general range of EVI value is usually between -1 and +1. It can be calculated

using Equation (3) as mentioned below:

$$EVI = G * \frac{(\rho_{\text{NIR}} - \rho_{\text{red}})}{(\rho_{\text{NIR}} + C1 * \rho_{\text{red}} - C2 * \rho_{\text{blue}} + L)} \quad (3)$$

where G is a gain factor, L is a soil adjustment, C1 and C2 are coefficients for corrections for atmospheric conditions [32].

Table 3. NDVI, EVI, and NDWI classification

Class-NDVI	Classification Criterion	Class-NDWI	Classification Criterion
Water, No vegetation, Bare soil,	NDVI $\leq$ 0	Very Low (Drought, Surface without water)	NDWI $\leq$ -1
Very Low vegetation	$\leq$ 0.2	Moderately Drought	-0.3 to 0.0
Low to Moderately Low	0.2 < NDVI $\leq$ 0.6	Flooding and Moisture	0.0 to 0.2
Moderately High to Very High (Thick Forest/Vegetation)	0.6 < NDVI $\leq$ 1	Surface water	0.2 to 1

4 Results and Discussion

In the area of the Mangura Nala watershed, NDWI, NDVI, and EVI consistently obtained substantial accuracy, according to the findings of various methodologies, months, visual analysis, and investigation. To properly examine rainfall using NDWI and EVI patterns and their relationships, the resulting thematic images have been imported into ArcGIS 10.4 and ERDAS Imagine. The generated maps, which are shown in Figures 3, 4 and 5, show the quantity of vegetation based on NDVI, EVI, and other metrics, as well as the geographical distribution of the annual rainfall means from 2013 to 2023.

4.1 Temporal variation of rainfall in the watershed

The temporal map of precipitation for 15 stations in the Mangura Nala watershed was created using a bar graph. The respective period of variation of precipitation was considered against each rain Gauge station. The temporal fluctuation of rainfall in and around the Mangura Nala watershed varies from station to station. We chose 15 rain gauge sites based on Earth data climatic location, as shown in Figure 2. The average rainfall from Amethi to Chapri stations is more than 900mm, with the pre-monsoon having lower rainfall than the post-monsoon. The monsoon season brings the most rainfall. In comparison to the rest of the station, Bhodh Chak and Burhgharea received the most rainfall. The temporal variance of rainfall in 2013 is greater compared to other periods in the monsoon, roughly 2750 mm in August at the Burhgharea station. The seasonality of rainfall in 2019 and 2020 is larger compared to previous periods in the monsoon, is about 2000 mm in Bhod Chack, Bhagawanpur stations, and Burhgharea stations from June to September. The seasonality of rainfall variation in the entire watershed has a direct impact on the vegetation and water bodies.

4.2 Vegetation Dynamics Estimation

Using the NDVI, the relationship between spectral vegetative variability and variations in vegetation growth rate was thoroughly investigated. The results of this study demonstrated that NDVI values differed with time. Table 4 and Figures 3 and 4 indicate the spatio-temporal variation of NDVI and EVI from 2013 to 2023. Vegetation indices have shown a significant influence on rainfall averages. The high NDVI suggests a more sustainable climate for photosynthesis.

4.3 Rainfall deviation pattern with vegetation (NDVI and EVI)

An overview of the overall rainfall distribution is provided by the average rainfall for the year from 2013 to 2023 (Figure 2). Any departure from this means or the appropriate season is crucial since it provides information on the overall biomass and the health of the plants. The surface vegetation region's pre-monsoon NDVI values ranged from 0.9 to -0.20. The 2013 monsoon season had the most surface vegetation cover (0.99), followed by the post-monsoon season (0.97) and the pre-monsoon season (0.91), showing that 2013 had the most surface vegetation cover during the monsoon season. From 2015 to 2021, the monsoon season had the greatest average vegetation surface value, ranging from 0.98 to 0.96. When compared to prior study years, the lowest NDVI value in 2021 was -0.19 during the monsoon season, while the highest value during the monsoon season was around 0.98. The Mangura Nala watershed in general shows an increase in vegetation growth during the monsoon season except in the north-western portion, which comprises of hilly region. The spatial distribution makes it evident that areas with high NDVI and EVI are primarily covered by dense vegetation (Figures 3 and 4). Due to the establishment of the seasonal crop primarily in plain areas, the monsoon NDVI has an excellent NDVI distribution in most regions (Figure 3). In 2013, the surface vegetation region acquired pre-monsoon EVI values ranging from 0.60 to 0.09. The 2013 monsoon season showed 0.95 to 0.01, while the post-monsoon showed 0.45 to 0.10, indicating that 2013 experienced higher surface vegetation cover during the monsoon season.

Table 4. NDVI, EVI, and NDWI classification Values

	Period	NDVI-max	NDVI-min	NDWI -max	NDWI -min	EVI - max
2013	Pre-monsoon (January –May)	0.91	-0.20	0.89	-0.20	0.60
	Monsoon (June –September)	**0.99**	-0.20	**0.99**	-0.20	**0.95**
	Post-monsoon (October –December)	0.97	-0.20	0.96	-0.20	0.45
2015	Pre-monsoon (January –May)	0.93	-0.20	0.84	-0.20	0.94
	Monsoon (June –September)	**0.98**	-0.20	**0.98**	-0.20	**0.95**
	Post-monsoon (October –December)	0.96	-0.20	0.90	-0.20	0.35
2017	Pre-monsoon (January –May)	0.91	-0.20	0.87	-0.20	0.91
	Monsoon (June –September)	**0.96**	-0.20	**0.97**	-0.20	**0.99**
	Post-monsoon (October –December)	0.94	-0.20	0.91	-0.20	0.42
2019	Pre-monsoon (January –May)	0.93	-0.20	0.72	-0.20	0.94
	Monsoon (June –September)	**0.97**	-0.20	**0.93**	-0.20	**0.97**
	Post-monsoon (October –December)	0.95	-0.20	0.89	-0.20	0.66
2021	Pre-monsoon (January –May)	0.89	-0.20	0.89	-0.20	0.81
	Monsoon (June –September)	**0.98**	**-0.19**	**0.97**	-0.20	**0.96**
	Post-monsoon (October –December)	0.92	-0.20	0.96	-0.20	0.38
2023	Pre-monsoon (January –May)	0.94	-0.20	0.86	-0.20	0.71
	Monsoon (June –September)	**0.96**	**-0.19**	**0.98**	-0.20	**0.89**
	Post-monsoon (October –December)	0.91	-0.20	0.94	-0.20	0.50

Bold letters indicate Maximum and Minimum values in the indices.

Figure 4 and Table 4 depict the spatio-temporal variability of seasonal changes. From 2013 to 2023, the monsoon season has shown the highest vegetation indices. When compared to other research years, the lowest EVI value in 2015 was -0.02 during the pre-monsoon season. Whereas the maximum value during the monsoon season was approximately 0.99 in 2017. Overall, EVI maximum values during the monsoon season were around 0.99, whereas post-monsoon seasons ranged from 0.35 to 0.66. Similarly, the EVI with positive deviation demonstrates an excellent crop pattern, which is also strongly supported by the positive rainfall deviation distribution.

4.4 Spatiotemporal dynamics Rainfall variation pattern with surface water NDWI (Water bodies)

Normalized Difference Water Index (NDWI) was used to examine the temporal and spatial variability of surface water. McFeeters (1996) states that values greater than 0 signify that water covers the area. The accuracy evaluation showed that the Mangura River sub-basins' surface water bodies were successfully captured by the NDWI. Table 4 displays the NDWI values, which were obtained from the analysis for the years 2013-2023. In general, the NDWI and ground-truthing data showed full agreement. These findings are in line with several studies that showed the good performance and dependability of NDWI in mapping surface water bodies. Significant temporal fluctuations in the watershed surface water area are revealed by the NDWI results in Figure 5. In 2013, the region covered by surface water experienced pre-monsoon NDWI ranging from -0.20 to 0.89. The 2013 monsoon season showed -0.20 to 0.99, while the post-monsoon showed -0.20 to 0.96, indicating that 2013 recorded the highest surface water cover during the monsoon season. Figure 5 and Table 4 indicate the respective years' data and changes. In 2013, the monsoon season has the maximum water surface value of around 0.99. In 2021 and 2023, this area shows maximum values in the monsoon and post-monsoon seasons of 0.97 to 0.98 and 0.96 to 0.94, respectively. In the Mangura watershed region, variations in surface water are generally closely related to patterns of rainfall. However, this link has become more intense in the 15 rain gauge stations of Mangura watershed due to changes in land use and rainfall variation in the area.

Notably, natural terrain is fast being converted into agricultural and urban areas, resulting in less water reaching the subsurface to replenish aquifers and maintain stream baseflow. As a result, surface water bodies are becoming increasingly dependent on rainfall-driven runoff. The impact of rainfall on water bodies was assessed using the rainfall deviation method. The image includes clouds, although their impact on water extraction is minimal. As shown in Figure 5, NDWI computation can identify areas with higher concentrations than water because of the cloud's reflectance. The experimental approach is like that of an urban river area, as the shadows cast by clouds align with the solar azimuth. Figures 3, 4 and 5 depict the entire method,

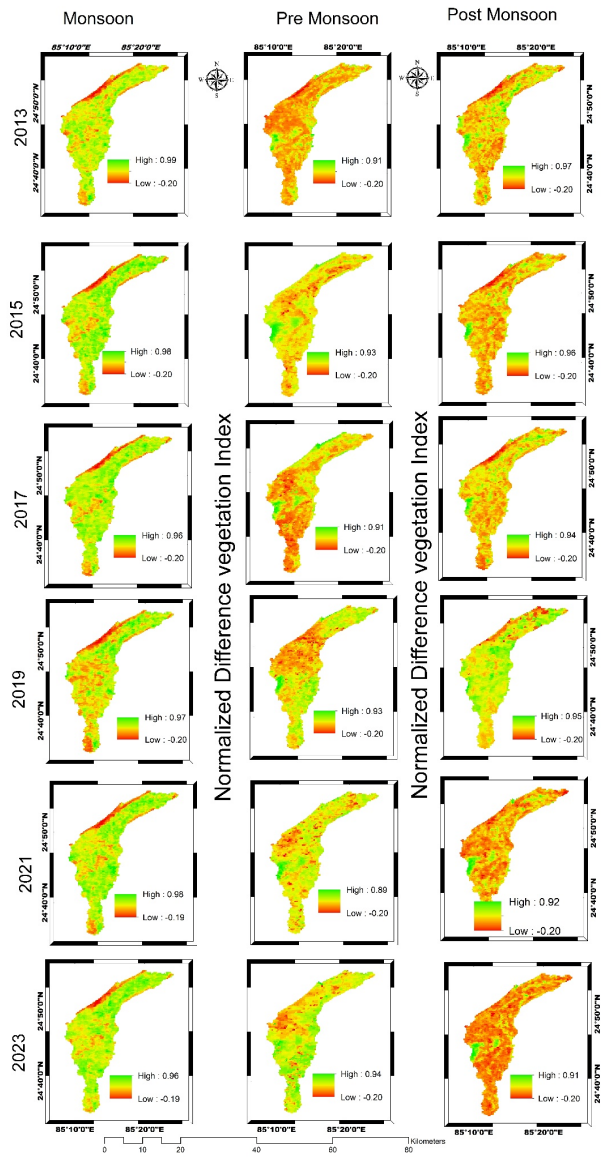

Fig. 3. Spatial and temporal variation of NDVI

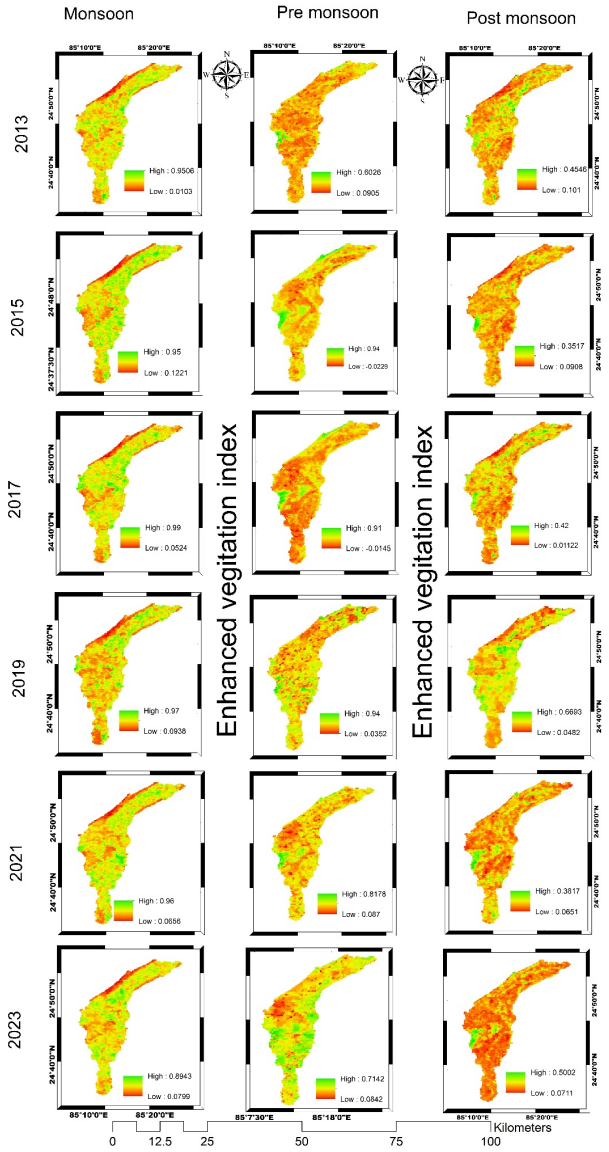

Fig. 4. Spatial and temporal variation of EVI

while Tables 2 and 3 show the experiment's accuracy. These results offer significant new information for the watershed's environmental preservation, agricultural planning, and water resource management. The regional variability of drought intensity identifies regions that may benefit from focused efforts to lessen the effects of the drought and allow for more intelligent resource allocation. In this regard, framing policies in liaison with the prevailing conditions can help in ensuring adequate supply of drinking water as well as to maintain agricultural productivity, ultimately aiming towards a sustainable and climate-resilient future in the study area.

5 Conclusion

Monitoring precipitation patterns and assessment through indices such as NDVI and NDWI provides real-time, both quantitative and qualitative data for policymakers. High correlation of NDVI and rainfall distribution has been observed during the monsoon season, while it is not the case during the pre-monsoon season. An understanding of the deviation in precipitation patterns during the pre-monsoon and monsoon seasons is significant for estimating the drought-prone areas and areas which produce a lot of crops. These findings can be well employed for water resource management, agricultural planning, and environmental conservation in the watershed. Resource allocation can be made more effective and justified

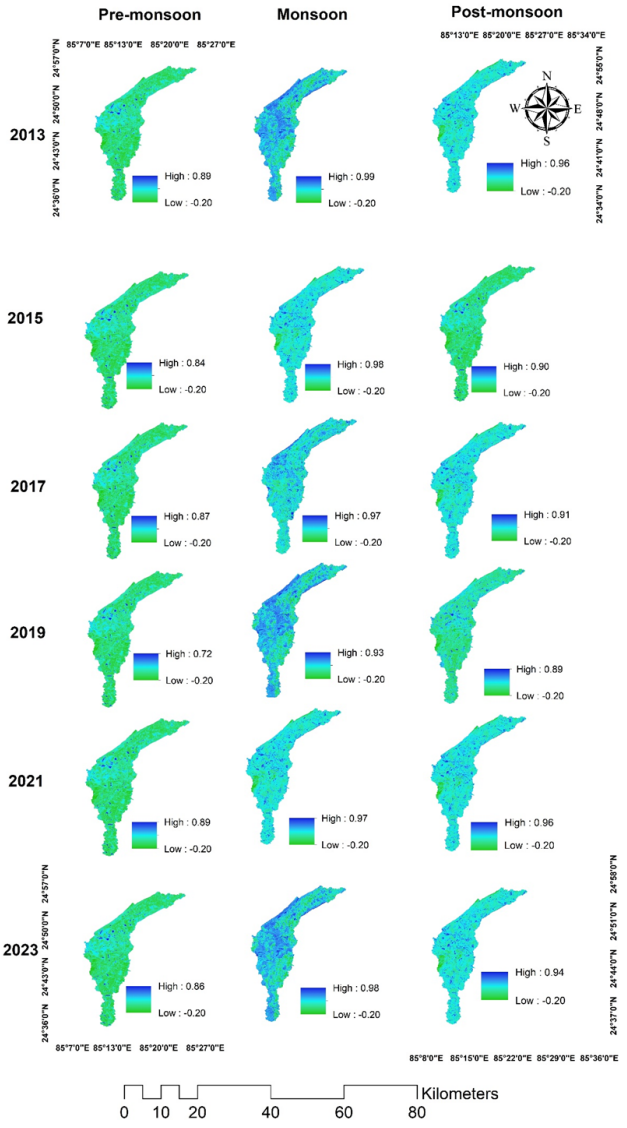

Fig. 5. NDWI Map of Mangura Nala watershed from 2013-2023

based on such a study, especially in areas with high drought intensity. Quantitative information about inter-annual variations during the summer and monsoon seasons and their relationship to rainfall is provided by the percent NDVI deviation, which displays percentage increases or decreases relative to the average. To better understand ecological deviations caused by climate change, further research on the relationship between vegetation and climate is required.

References

1) Islam T, Rico-Ramirez MA, Han D, Srivastava PK, Ishak AM. Performance evaluation of the TRMM precipitation estimation using ground-based radars from the GPM validation network. *Journal of Atmospheric and Solar-Terrestrial Physics*. 2012;77:194–208. Available from: https://dx.doi.org/10.1016/j.jastp.2012.01.001.
2) Gajbhiye S, Meshram C, Singh SK, Srivastava PK, Islam T. Precipitation trend analysis of Sindh River basin, India, from 102-year record (1901–2002). *Atmospheric Science Letters*. 2016;17(1):71–77. Available from: https://dx.doi.org/10.1002/asl.602.
3) Sruthi S, Aslam MAM. Agricultural Drought Analysis Using the NDVI and Land Surface Temperature Data; a Case Study of Raichur District. *Aquatic Procedia*. 2015;4:1258–1264. Available from: https://dx.doi.org/10.1016/j.aqpro.2015.02.164.
4) Srivastava PK, Han D, Rico-Ramirez MA, Islam T. Sensitivity and uncertainty analysis of mesoscale model downscaled hydro-meteorological variables for discharge prediction. *Hydrological Processes*. 2014;28(15):4419–4432. Available from: https://dx.doi.org/10.1002/hyp.9946.
5) Mohammed-Aslam MA, Rizvi SS. Hydrogeochemical characterisation and appraisal of groundwater suitability for domestic and irrigational purposes in a semi-arid region, Karnataka state, India. *Applied Water Science*. 2020;10(12):237. Available from: https://dx.doi.org/10.1007/s13201-020-01320-1.
6) Harishnaika N, Ahmed SA, Kumar S, Arpitha M. Spatio-temporal rainfall trend assessment over a semi-arid region of Karnataka state, using non-parametric techniques. *Arabian Journal of Geosciences*. 2022;15(16):1392. Available from: https://dx.doi.org/10.1007/s12517-022-10665-7.
7) Warsi T, Mukherjee S, Biswas G, Mitran T, Rizvi SS. Urban water resources and its sustainable management. *Current Directions in Water Scarcity Research*. 2022;6:489–509. Available from: https://doi.org/10.1016/B978-0-323-91838-1.00020-8.
8) Mukherjee S, Rizvi SS, Biswas G, Paswan AK, Vaiphei SP, Warsi T, et al. Aquatic Eco-systems Under Influence of Climate Change and Anthropogenic Activities: Potential Threats and Its Mitigation Strategies. In: Hydrogeochemistry of Aquatic Ecosystems. 2023;p. 307–331. Available from: https://doi.org/10.1002/9781119870562.ch14.
9) Sultana T, Hegde S, Warsi T, Tahama K, Rizvi SS, Mukherjee S, et al. Data analytics for drought vulnerability under climate change scenarios. In: Data Analytics and Artificial Intelligence for Earth Resource Management. Elsevier. 2025;p. 137–156. Available from: https://doi.org/10.1016/B978-0-443-23595-5.00008-5.
10) Ashok K, Guan Z, Saji NH, Yamagata T. Individual and Combined Influences of ENSO and the Indian Ocean Dipole on the Indian Summer Monsoon. *Journal of Climate*. 2004;17(16):3141–3155. Available from: https://dx.doi.org/10.1175/1520-0442(2004)017<3141:iacioe>2.0.co;2.
11) Dash SK, Jenamani RK, Kalsi SR, Panda SK. Some evidence of climate change in twentieth-century India. *Climatic Change*. 2007;85(3-4):299–321. Available from: https://dx.doi.org/10.1007/s10584-007-9305-9.
12) Mondal A, Khare D, Kundu S. Spatial and temporal analysis of rainfall and temperature trend of India. *Theoretical and Applied Climatology*. 2015;122(1-2):143–158. Available from: https://dx.doi.org/10.1007/s00704-014-1283-z.
13) Harishnaika N, Ahmed SA, Kumar S, Arpitha M. Computation of the spatio-temporal extent of rainfall and long-term meteorological drought assessment using standardized precipitation index over Kolar and Chikkaballapura districts, Karnataka during 1951-2019. *Remote Sensing Applications: Society and Environment*. 2022;27:100768. Available from: https://doi.org/10.1016/j.rsase.2022.100768.
14) Kokaly RF, Despain DG, Clark RN, Livo KE. Mapping vegetation in Yellowstone National Park using spectral feature analysis of AVIRIS data. *Remote Sensing of Environment*. 2003;84(3):437–456. Available from: https://dx.doi.org/10.1016/s0034-4257(02)00133-5.
15) Guo B, Zhou Y, Wang SX, Tao HP. The relationship between normalized difference vegetation index (NDVI) and climate factors in the semiarid region: A case study in Yalu Tsangpo River basin of Qinghai-Tibet Plateau. *Journal of Mountain Science*. 2014;11(4):926–940. Available from: https://dx.doi.org/10.1007/s11629-013-2902-3.

16) Yang X, Yang T, Ji Q, He Y, Ghebrezgabher MG. Regional-scale grassland classification using moderate-resolution imaging spectrometer datasets based on multistep unsupervised classification and indices suitability analysis. *Journal of Applied Remote Sensing*. 2014;8(1):083548. Available from: https://dx.doi.org/10.1117/1.jrs.8.083548.
17) Ogutu JO, Piepho HP, Dublin HT, Bhola N, Reid RS. El Niño–Southern Oscillation, rainfall, temperature and Normalized Difference Vegetation Index fluctuations in the Mara-Serengeti ecosystem. *African Journal of Ecology*. 2008;46(2):132–143. Available from: https://dx.doi.org/10.1111/j.1365-2028.2007.00821.x.
18) Wang J, Rich PM, Price KP. Temporal responses of NDVI to precipitation and temperature in the central Great Plains, USA. *International Journal of Remote Sensing*. 2003;24(11):2345–2364. Available from: https://dx.doi.org/10.1080/01431160210154812.
19) Nemani RR, Keeling CD, Hashimoto H, Jolly WM, Piper SC, Tucker CJ, et al. Climate-Driven Increases in Global Terrestrial Net Primary Production from 1982 to 1999. *Science*. 2003;300(5625):1560–1563. Available from: https://dx.doi.org/10.1126/science.1082750.
20) Raghavendra BR, Aslam MAM. Sensitivity of vegetation indices of MODIS data for the monitoring of rice crops in Raichur district, Karnataka, India. *The Egyptian Journal of Remote Sensing and Space Science*. 2017;20(2):187–195. Available from: https://dx.doi.org/10.1016/j.ejrs.2016.06.005.
21) Goward SN, Tucker CJ, Dye DG. North American vegetation patterns observed with the NOAA-7 advanced very high resolution radiometer. *Vegetatio*. 1985;64(1):3–14. Available from: https://dx.doi.org/10.1007/bf00033449.
22) Tucker CJ, Sellers PJ. Satellite remote sensing of primary production. *International Journal of Remote Sensing*. 1986;7(11):1395–1416. Available from: https://dx.doi.org/10.1080/01431168608948944.
23) McFeeters SK. The use of the Normalized Difference Water Index (NDWI) in the delineation of open water features. *International Journal of Remote Sensing*. 1996;17(7):1425–1432. Available from: https://dx.doi.org/10.1080/01431169608948714.
24) Luo JC, Sheng YW, Shen ZF, Li JL, Gao LJ. Automatic and high-precise extraction for water information from multispectral images with the step-by-step iterative transformation mechanism. *Journal of Remote Sensing*. 2009;13(4):610–615. Available from: https://scholar.google.com/citations?view_op=view_citation&hl=en&user=7OCF0kIAAAAJ&citation_for_view=7OCF0kIAAAAJ:mvPsJ3kp5DgC.
25) Ashtekar AS, Mohammed-Aslam MA, Moosvi AR. Utility of Normalized Difference Water Index and GIS for Mapping Surface Water Dynamics in Sub-Upper Krishna Basin. *Journal of the Indian Society of Remote Sensing*. 2019;47(8):1431–1442. Available from: https://dx.doi.org/10.1007/s12524-019-01013-6.
26) Rizvi SS, Aslam M. Estimation of hypsometric integral and groundwater potential zones of Amarja Reservoir Catchment, Karnataka, India using SRTM data and geospatial tools. *International Journal of Economic and Environment Geology*. 2018;9(2):75–85. Available from: https://doaj.org/article/5408aff7044b45c2bdce85b9cad519d9.
27) Shalini, Kommineni HR, Jeelani SH, Jaragapu DCK, Rizvi SS. Land use landcover and accuracy evaluation using remote sensing and GIS in and around Vijayawada city Andhra Pradesh, India. *AIP Conference Proceedings*. 2023;2759:020005. Available from: https://doi.org/10.1063/5.0146411.
28) Mohanta T, Rizvi SS, Mohammed-Aslam MA, Jeelani SH. Mapping of LULC change detection using remote sensing and GIS in Kalaburagi district, Karnataka, India. In: AIP Conference Proceedings;vol. 2759. AIP Publishing. 2023;p. 020006. Available from: https://doi.org/10.1063/5.0144299.
29) Chen XL, Zhao HM, Li PX, Yin ZY. Remote sensing image-based analysis of the relationship between urban heat island and land use/cover changes. *Remote Sensing of Environment*. 2006;104(2):133–146. Available from: https://dx.doi.org/10.1016/j.rse.2005.11.016.
30) Gao BC. NDWI—A normalized difference water index for remote sensing of vegetation liquid water from space. *Remote Sensing of Environment*. 1996;58(3):257–266. Available from: https://doi.org/10.1016/S0034-4257(96)00067-3.
31) Arpitha M, Ahmed SA, Harishnaika N. Land use and land cover classification using machine learning algorithms in google earth engine. *Earth Science Informatics* . 2023;16:3057–3073. Available from: https://doi.org/10.1007/s12145-023-01073-w.
32) Gaznayee HAA, Al-Quraishi AMF, Mahdi K, Ritsema C. A Geospatial Approach for Analysis of Drought Impacts on Vegetation Cover and Land Surface Temperature in the Kurdistan Region of Iraq. *Water*. 2022;14(6):927. Available from: https://dx.doi.org/10.3390/w14060927.